Pergamon

Cement and Concrete Research, Vol. 27, No. 7, pp. 1061-1072, 1997

0008-8846/97 $17.00 + .00

PII S0008-8846(97)00093-8

ETTRINGITE FORMATION IN LOW C_3A PORTLAND CEMENT EXPOSED TO SODIUM SULFATE SOLUTION

M.A. González and E.F. Irassar
Departamento de Construcciones
Facultad de Ingeniería
Universidad Nacional del Centro
7400-Olavarría, Argentina

(Refereed)
(Received September 25, 1996; in final form May 9, 1997)

ABSTRACT

Four low-C_3A Portland cements with different C_3S content (40 to 74%) were stored for two years in sodium sulfate solution. Expansion and flexural strength were monitored as mechanical properties, while the microstructural changes were studied by X-ray diffraction and scanning electron microscopy using X-ray microanalysis. For this cement type, the alteration processes can be described by three stages: induction, gypsum formation and delayed ettringite formation. The results shown that delayed ettringite is derived from ferroaluminate phases and it was found for all cements. The great expansion was measured for high C_3S-content cement and the expansive formation of ettringite in this case was attributable to localized gypsum formation. © *1997 Elsevier Science Ltd*

Introduction

After 1930, the sulfate resistance of portland cements was closely related with the C_3A content. Cement standards of the world (ASTM, AFNOR, BS and DIN) recognized the preponderant role of alumina bearing phases, thus its content was limited for sulfate resistant Portland cements (1). However, C_3A-content is not the only factor of cement composition influencing durability in sulfate environments. It has been observed that for the same C_3A-level, the rate of deterioration of cements can differ, depending on the manufacturing processes of clinkers (2,3) and the crystalline form of the C_3A (4). Ettringite formation derived from ferroaluminate phase has also been assumed as a potential sulfate deterioration problem (5).

On the other hand, the C_3S-content was considered an important parameter on sulfate resistance of Portland cement, too. The increase of C_3S-content implies an increase of the CH liberated during the hydration of portland cement and modifies the development of strength, heat and porosity of the hardened paste. In sulfate environment, CH can convert to gypsum leading to surface damage of the softening-spalling type, mass loss and strength retrogression. But, it is not well established that gypsum formation leads to expansion (6).

Literature review (8-13) has shown more suggestions and contradictions than facts about the role of C_3S content on sulfate resistance of Portland cement. European and USA standards do not provide any limitation for C_3S content, while the cement standard throughout the ex-Soviet countries adopted certain limits for C_3S content (i.e., STAS 3011-76, GOST 22266-76) (1).

The objective of this study was to relate the mechanical behavior with the microstructural changes of very low-C_3A cement with C_3S content variable using mortar bars immersed in sodium sulfate solution for two years.

Experimental

Materials. Four Type V Portland cements, with very low C_3A and different C_3S content, were used in this experimental program. Chemical composition and physical properties of cements used are given in Table 1. Cements are designated as PC40, PC50, PC60 and PC74 accordingly their C_3S content. The chemical composition was determined by X-ray fluorescence and the XRD analysis of cements confirmed the absence of C_3A. All cements have the same fineness (specific surface Blaine) and the evolution of strength was quite different up to seven days. However, C_3S level had little influence on 28 days' compressive strength.

TABLE 1

Composition and Physical Characteristic of Portland Cements

	PC40	PC50	PC60	PC74
Oxide composition, percent by weight				
SiO_2	23.66	22.93	22.35	21.00
Al_2O_3	3.00	3.09	3.17	3.29
Fe_2O_3	5.41	5.19	4.97	4.68
CaO	62.14	63.53	64.92	66.00
MgO	0.60	0.62	0.63	0.67
SO_3	1.59	1.77	1.96	2.20
Alkalis	1.61	1.50	1.38	1.23
Loss by Ignition	1.61	1.50	1.38	1.23
Calculated composition, percent by weight				
C_3S	40	50	60	74
C_2S	38	28	18	4
C_3A	0	0	0	1
C_4AF	15	15	15	14
Fineness Blaine, m^2/kg	313	311	309	306
Compressive Strength (ASTM C 349) in MPa				
3 days	11.4	16.0	21.7	27.3
7 days	17.6	24.5	27.2	29.2
28 days	32.7	33.5	32.7	32.5
Expansion in percent (ASTM C 452)				
14 days	0.015	0.013	0.014	0.012
90 days	0.025	n.d.	n.d.	0.021
360 days	0.030	n.d.	n.d.	0.045

n.d. = not determined

According to ASTM C 150, all cements should be considered as sulfate resistant, because the expansion at 14 days was lower than 0.040% when they were testing according to ASTM C 452.

Procedures

For each cement, sixteen mortar bars were cast according to ASTM C 1012 (25 × 25 × 285 mm, cement:sand ratio 1:2.75 and w/c = 0.485) and stored in the moist cabinet during 24 hours. The specimens were removed from the mold and cured in saturated lime-water solution for 28 days. Thereafter, the bars were immersed in plastic storage tanks containing the sodium sulfate solution (0.35 M or 5% Na_2SO_4). The volume proportion of sulfate solution to mortar bars was maintained at 4 to 1 throughout the test. At the exposure time, the same level of maturity (judged by compressive strength) was achieved for all cements. Everyday, the sulfate solution was agitated and manually titrated with a combined solution (H_2SO_4 2 N and Na_2SO_4 0.35 M) to maintain the pH, and the consumption of titration solution was registered. A few drops of phenolphthalein were added in each tank as pH-indicator.

At 28, 56, 90, 180, 365, 540 and 720 days of sulfate immersion, the specimens were tested to determine the expansion and flexural strength of mortar. Flexural strength test was conducted on bars using a center-point loading and a span length/deep relation of 2.5. At each test age, two bars were tested and five values of strength were determined for each bar. The expansion was measured on the remaining specimens and the visual aspect was judged, too.

A similar series was stored in lime saturated water and the same properties were evaluated as reference values.

The change in mineralogical phases of the mortars was evaluated by XRD analysis using a powdered sample. Measurements were performed on a diffractometer (Philips X'Pert) using Cu Kα radiation and operating at 40 kV and 20 mA. Step scanning was used with a

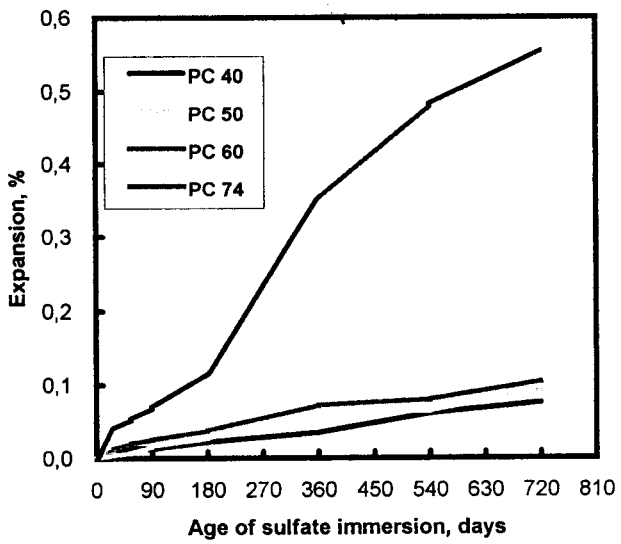

FIG. 1.
Expansion of mortars with different C_3S-content Type V portland cements.

scan speed of 2°/min and sampling interval of 0.02°2θ. Fragment of bars broken off and washed with acetone were examined by SEM equipped with energy dispersed X-ray analysis (EDXA).

Results

Expansion. Figure 1 shows the data on expansion in Type V cement exposed to sulfate solution. These data indicate higher expansion for specimens with PC74 cement for all test ages. PC74 mortar reached an expansion of 0.117% at 180 days of exposure overcoming the limit proposed by Patzias (14) for Type II cement. For the three other cements, the expansion remained in the order of 0.022 to 0.037% and these values are lower than the proposed limits for sulfate resistant portland cement (0.050%)(14).

The curves indicate that the expansion rate decreases for the PC40, PC50 and PC60 during all test ages. However, the expansion rate in PC74 mortar shows a trend similar to other mortars until 180 days and thereafter it increases suddenly.

Flexural Strength. Data on evolution of the relative initial (28 days water cured) flexural strength in sulfate are shown in Figure 2. They show a typical behavior in sulfate solution: there is a strong increase of strength during the first six months and then it remains constant or decreases slowly.

For PC40, PC50 and PC60 cements, the flexural strength in sulfate solution was higher than flexural strength in water during one year ($f_{sulfate}/f_{water}$ = 1.18 to 1.44). The strength in sulfate solution increased up to 180 days, beyond that the strength was approximately constant or decreased slowly.

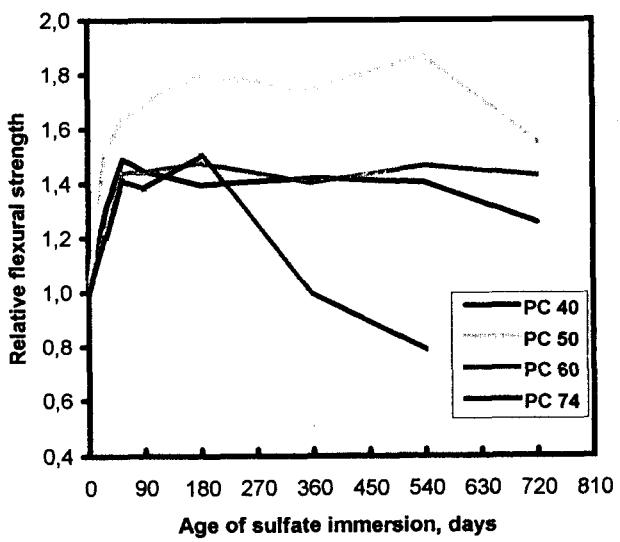

FIG. 2.
Variation of relative flexural strength of portland cement mortars.

On the contrary, the PC74 showed a gradual loss of relative strength after 180 days in sulfate environment. At 360 days, strength was lower than that control specimens in water ($f_{sulfate}/f_{water} = 0.71$).

Visual Aspect. After 28 days of sulfate immersion, PC60 and PC74 prisms showed signs of superficial softening. At this stage, the outer layer of paste came off and the surface of specimens had a sandy appearance. Cracks at the corners and edges were observed at 56 days. Then, it progressed and the corners were found severely corroded at one year. For PC60, the deterioration of specimen corners was less pronounced than the corresponding prisms made using PC74. The great expansion of PC74 mortar produced the curvature of the prisms.

Regarding to other cements, PC40 and PC50 prisms showed only a slight scaling of the paste after two years in sulfate immersion.

Solution Consumption. Figure 3 shows the cumulative titration-solution added during time for mortars with low C_3A. Mortar with CP74 required more solution than the other cements. The rate of consumption decreased throughout the time for all cements.

XRD Analysis. For all cements, the XRD patterns up to 720 days of sulfate exposure are shown in Figure 4. During the first three months, minor differences were only detected by XRD analysis in all samples. For all cements, the gypsum formation ($2\theta = 11.60$) was detected after 90 days of sulfate immersion and it was always present in all mortar at later test age. The intensity of CH peak ($2\theta = 18.02$) was very strong for all cement at all test ages.

The great difference in mineralogical phases was the ettringite formation ($2\theta = 9.08$) after 360 days of sulfate exposure for PC74 mortar. Thereafter, its peak intensity increased. For

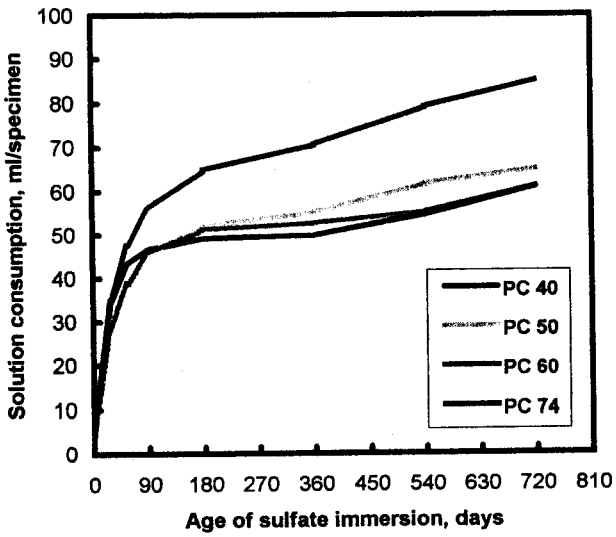

FIG. 3.
Cumulative solution consumption for mortar-solution system.

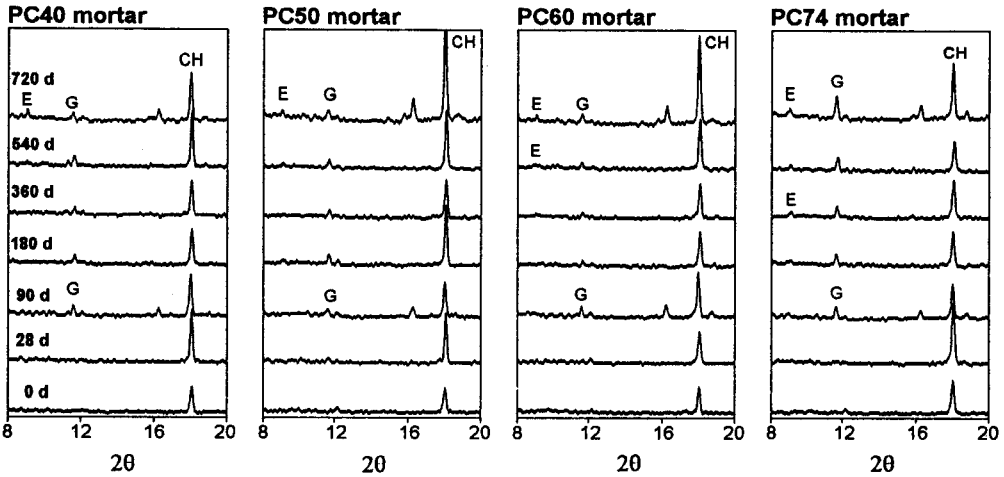

FIG. 4.
X-ray diffractograms of portland cement mortars at each test age. (E = ettringite, G = gypsum and CH = calcium hydroxide).

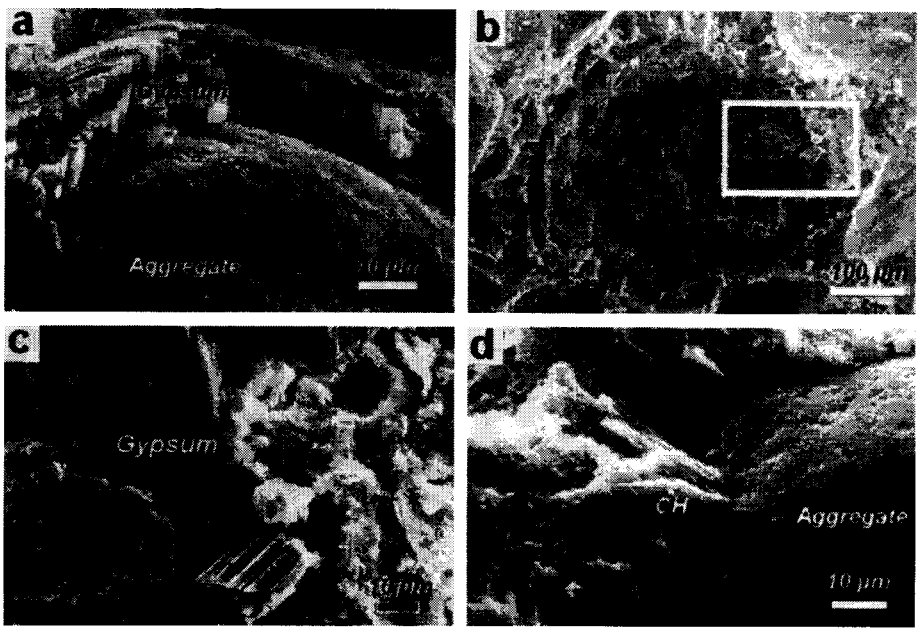

FIG. 5.
SEM micrographs of mortars: (a) Gypsum crystals grown in paste-aggregate interface in PC74 mortar at 360 days. (b) Air void covered by a gypsum skin in PC74 mortar at 360 days. (c) Detail of b. (d) Calcium hydroxide around aggregate in PC40 mortar at 360 days.

PC60, it was detected at 540 days with very low intensity peak and with a well defined peak at 720 days. For the PC40 and PC50, ettringite was detected at two years.

SEM Observation. For the CP74 mortar, SEM observation on specimens after 360 days in sulfate solution showed the formation of gypsum crystal deposited preferably around the aggregates (Fig. 5a) and air voids (Fig. 5b and 5c). Gypsum crystals grown perpendicular to aggregate face or void walls forming a skin of 20 to 50 μm thick. On the other hand, PC40 and PC50 mortar after 360 days of sulfate immersion showed CH deposit around aggregates

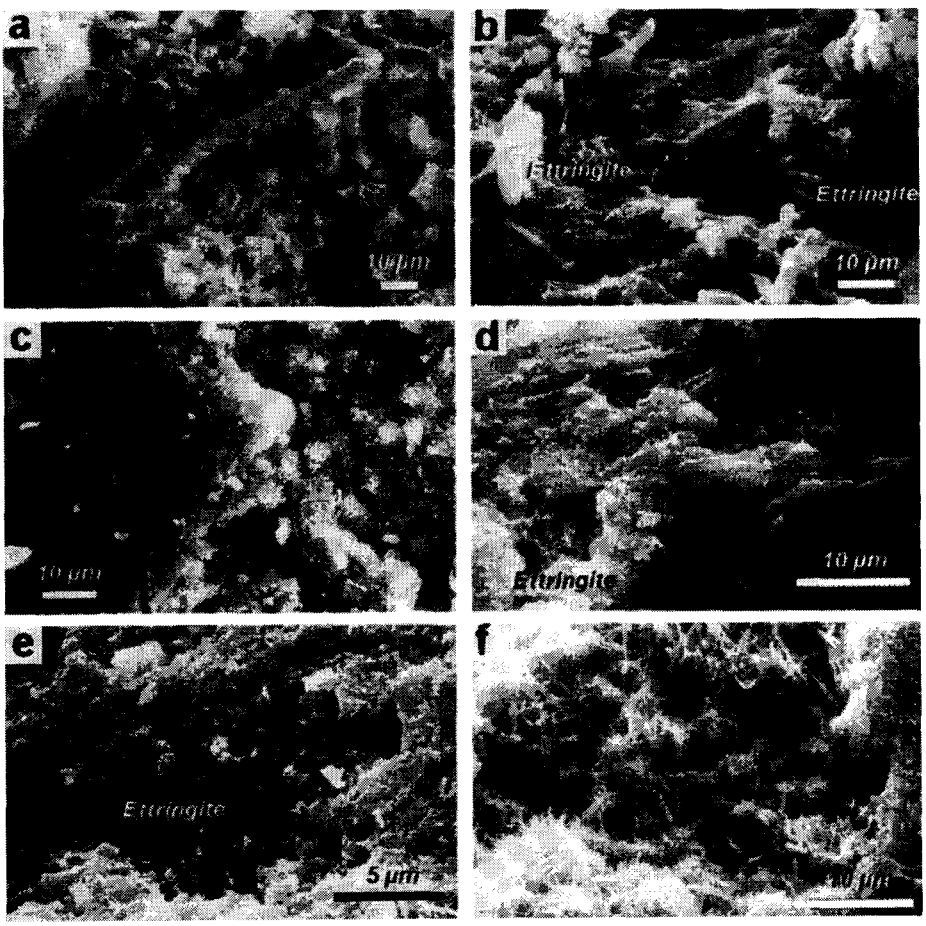

FIG. 6.

SEM micrographs of mortars: (a) Ettringite in free needles form (C = 63.2%, A = 10.2%, F = 1.8%, $\overline{S}$ = 17.6%) in PC74 mortar at 360 days. (b) Ettringite in package form (C = 75%, A = 7.3%, F = 3.2%, $\overline{S}$ = 14.5%) in PC74 mortar at 360 days. (c) Ettringite into the paste for PC60 mortar at 540 days (C = 58.5%, A = 6.4%, F = 9.8%, $\overline{S}$ = 13.8%). (d) Cluster of ettringite at air void in PC40 at 720 days (C = 56%, A = 3.4%, F = 6.3%, $\overline{S}$ = 14.7% and $\overline{S}$ = 19.1%). (e) Cluster of ettringite at air void in PC50 at 720 days. (f) Generalized formation of ettringite in PC74 mortar at 720 days. (C = 51%, A = 7.1%, F = 6.1%, $\overline{S}$ = 21.8 %).

near the surface of specimens (Fig. 5d) and the gypsum formations were not highly localized.

At 360 days, the ettringite was observed in PC74 mortars with different morphology: free needles nearby of void pores (Fig. 6a) and forming packages (Fig. 6b). At 560 days, ettringite needles were observed in PC60 mortars (Fig. 6c), too.

After two years, some crystals of ettringite deposited only in pores were observed in PC40 (Fig. 6d) and in PC50 mortars (Fig. 6e) while the interfaces of paste-aggregate continued formed by calcium hydroxide at few millimeters of exposed surface. At this time, the PC74 mortar showed a generalized ettringite formation into the mass of mortar (Fig. 6f). The EDX analyses of ettringite crystals revel the presence of alumina (4 to 10%), ferrite (2 to 10%), calcium (56 to 68%), sulfate (10 to 18%) and silica (7 to 25%). The A/F ratio showed by individual EDXA ranges from 0.6 to 1.5.

This study of microstructure by means of SEM leads to results similar to those derived from XRD analyses.

DISCUSSION

The data provided above indicate that the sulfate attack on low C_3A Portland cements is a phenomenon involving several stages. According to the dominating mechanism in each stage, instead of the processes are simultaneous, it can be divided into three stages: induction, gypsum formation and ettringite formation.

The **first stage** of the attack is characterized by: there is a stronger sulfate demand with a declined rate, the flexural strength increases, the expansion is small with decreasing rate, and there are no changes in the visual appearance of specimens. The duration of this stage is suggested between 56 and 90 days for Portland cements used.

The stronger sulfate demand (Fig. 3) is related to the solubility of CH from specimen surfaces by a through solution mechanism (15). The consumption rate has a pronounced declining rate up to 90 days, when the mortar-solution system reaches the equilibrium. At this time, the sulfate demand was more than two third of the total consumption in two years. However, gypsum or ettringite formation was not detected by XRD during this time.

In this stage, flexural strength increased (Fig. 2) due to pore filled by products of attack and the contribution to hydration rate of portland cement grains (16). According to the thermodynamic theory (17), the expansion in sulfate environment is derived from crystallization pressure, which is the result of interaction between the solid products of the chemical reaction (gypsum or ettringite) and the cement paste. Consequently, expansion was not present in this stage because crystals grow in unconfined condition leading to decrease the porosity (16).

The **second stage** began when the mortar-solution system reached an equilibrium status. The sulfate demand increased very slowly, the demand-rate was constant, the flexural strength had no significantly change and the expansion was low.

This stage is governed by diffusion processes and the gypsum formation into the mortar as the XRD analysis revels. According to Mehta (18), gypsum crystallization begins when the ettringite crystallization ceases due to the deficient alumina supply of aluminate from the solid phase to the solution phase. For cements with low C_3A-content, the ettringite crystallization cannot be detected previous to gypsum formation, and gypsum prevails as the first product of chemical reaction. Recently, Gollop and Taylor (19) suggest that the sequence should be identical to Mehta's theory, but the reaction to form ettringite occurs only within

the cement paste, and the crystal of this compound is possible to have a submicrometer dimension.

After 90 days, XRD analyses showed the gypsum formation for all cements. The different behavior of mortars is attributable to the crystallization zone of this compound. For the CP74 and PC60, gypsum is preferably localized in voids and in the paste-aggregate zone (Fig. 5). Evidently, gypsum is formed from CH precipitated around aggregates during cement hydration and in air voids due to the space available. The preferred crystallization of gypsum in the transition zone is attributed to the availability of CH and the higher porosity of this zone (20). This observation shows the high susceptibilities of interface zone to sulfate attack.

Several authors (6,13,18,21) agree that gypsum formation leads to softening of the external layer of mortar while the interior of the matrix remains cohesive. This formation is responsible of edge and corner corrosion of specimens described in the visual aspect topic and recently modeled (19). As suspected by Cohen and Mather (6), the flexural strength does not reflect the early stage of softening-spalling type of sulfate attack, which can only be appreciated in visual appearance of mortar bars. It is not clear that gypsum formation is associated with expansion (6). Mehta (18) points out that gypsum formation is one of the principal causes of the expansion in sulfate environment. Rasheeduzzafar (22) supposes that the transformation of CH to gypsum around CSH gel reduces the intrinsic strength and stiffness of CSH gel surrounding expansive crystals.

The above opinions are based on chemical principles, but they overlook the structure of mortar. Mortar and concrete are more porous than paste due to the increase of porosity in the system paste-aggregate (23). The authors believe that the high expansiveness of PC74 mortar is produced by the massive deposition of gypsum in the interface zone. Restricted growth of gypsum crystal generates the crystallization pressure (17) that causes the cracking. Generalized gypsum formation within the CSH structure causes expansion by crystal growth in weakened mortar (24). For others mortars, the gypsum crystals observed by SEM have a micrometer dimension and they were found disseminated into the paste. Under this condition, it does not cause a measurable expansion.

The delayed formation of ettringite is the distinction of the **third stage** of attack. It occurs with no significant changes in sulfate demand, while the expansion rate enlarges and the flexural strength drop. This behavior is typical of mortar in sulfate environment due to ettringite formation associated with cracking.

During this stage, the sulfate demand has no significant changes and the sulfate consumption prior the significant expansion is around 50ml/specimen. Brown (15) and Fraay et al. (25) have observed the same behavior for other cement types and pointed out that a threshold-value is related with the solution pH and its sulfate concentration. After threshold-value for PC74 mortar, there is a correlation between the expansion and the strength drop.

This stage occurs when mortar presents a dominant gypsum environment due to the continuous removal of CH. Under this condition, Mehta (18) suggests that the CSH starts losing strength and stiffness, and the ettringite crystals become expansive. For the PC74 mortar, it begins at 180 days. XRD pattern reveals the presence of ettringite after 360 days and it occurs after 540 days for PC60 mortar. For PC40 and PC50, the presence of clusters of well-defined crystals of ettringite were only detected after 720 days. The crystal growth in the pores does not cause expansion due to the surrounding environment dominated by CH at this age.

The compositions of the cements used indicates that ettringite would be derived of calcium-alumina-ferrite phase. This phase produces ettringite during its hydration that transforms into monosulfate phases of similar structure where the aluminate is exchanged for

ferrite (26). In sulfate environment, the reaction of this compound is very slow, but the mechanism for the sulfate attack is expected to be the same as for the calcium-aluminate phase (27).

The presence of Fe in EDX analysis shows that ettringite crystals are formed from the ferrite phases. On the other hand, the inclusion of silica into the crystal indicates that the precursor of ettringite was closely mixed with CSH gel. Approximate calculations suggest that the tentative composition of the ettringite should be the type $C_3(A_x,F_y).3CSH_2.26H$.

Conclusions

The results provide the confirmation that ettringite formation occurs in low C_3A cements exposed to sodium sulfate solutions. The attack mechanism for this cements can be divided into three stages: induction, gypsum formation and delayed ettringite formation.

The process of ettringite formation is quite slow and it occurs for all used cements. However, for high C_3S cement it was accompanied with high expansion, which confirms the role of gypsum in ettringite expansion. The high expansion of these cements is associated with the highly located gypsum formation at interfaces of aggregate-paste that disrupts the mortar and the attack increases.

The presence of Fe and Al in crystal composition of delayed ettringite provides the evidence that it is derived from the ferroaluminate phases.

Finally, the deterioration of low C_3A Portland cements by sulfate attack is possible and the C_3S content plays a decisive role in the potential damage of these cements.

Acknowledgments

This work was financed by the Secretaria de Ciencia y Tecnica de la Universidad del Centro and the Comision de Investigaciones Cientificas de la Prov. de Buenos Aires (CIC) and the clinkers were kindly supplied by Loma Negra CIASA.

References

1. Cembureau, Cement Standards of the World, 1991.
2. M. Nadu, Proc. of 7th Int. Congress on the Chemistry of Cement, Paris, France, VII/95 (1980).
3. F.M. Lea, The Chemistry of Cement and Concrete, p.149, Edward Arnold, Ltd., London, 1970.
4. P.K. Mehta, Proc. of 7th Int. Congress on the Chemistry of Cement, Paris, France, 5, 575 (1980).
5. ACI Committee 201, ACI Materials Journal 88, 551 (1991).
6. M.D. Cohen and B. Mather, ACI Materials Journal 88, 62 (1991).
7. E.G. Swenson and C.J. Mackenzie, Performance of concrete, p. 3, Univ. of Toronto Press, Canada, 1968.
8. B.P. Bellport, Performance of concrete, p. 77, Univ. of Toronto Press, Canada, 1968.
9. F.M. Lea, The Chemistry of Cement and Concrete, p. 355, Edward Arnold, Ltd., London, 1970.
10. I. Biczock, Concrete Corrosion and Concrete Protection, p. 69 and 254, Ed. Urmo, Barcelona, Spain, 1972.
11. J. Calleja, Proc. 7th Int. Congress on the Chemistry of Cement, Paris, France, VII2/1 (1980).
12. D. Dimic and S. Droljc, Porc. 8th. Int. Congress on the Chemistry of Cement, Rio de Janeiro, Brazil, V, 195 (1986).
13. Rasheeduzzafar, ACI Materials Journal 89, 574 (1992).
14. T. Patzias, Cement, Concrete and Aggregates 13, 50 (1991).

15. P.W. Brown, Cement and Concrete Research 11, 719 (1981).
16. E.F. Irassar, Cement and Concrete Research 20, 209 (1990).
17. Xie Ping and J.J. Beaudoin, Cement and Concrete Research 22, 631 (1992).
18. P.K. Mehta, Cement and Concrete Research 13, 401 (1983).
19. R.S. Gollop and H.F.W. Taylor, Cement and Concrete Research 25, 1581 (1995).
20. A.M. Brandt, Cement-Based Composites: Materials, Mechanical Properties and Performance, p. 141, E&FN Spon, London, 1995.
21. P.S. Mangat and J.M. Khatib, ACI Material Journal 92, 542 (1995).
22. Rasheeduzzafar et al., ACI Material Journal 87, 114 (1990).
23. Wilson and Liu, Cement and Concrete Research 20, 227 (1990).
24. C.D. Lawrence, Magazine of Concrete Research 42, 249 (1990).
25. A. Fraay, A. Reigersman and J. de Pee, ACI SP 100, 2041 (1987).
26. M. Collepardi, S. Monosi and G. Moriconi, Cement and Concrete Research 9, 431 (1979).
27. L.O. Höglund, Cement and Concrete Research 22, 217 (1992).